

Measurement and Modeling of the Indirect Coupling of Lightning Transients into the Sago Mine

Matthew B. Higgins, *Member, IEEE*, Marvin E. Morris, Michele Caldwell, *Member, IEEE*,
and Christos G. Christodoulou, *Fellow, IEEE*

Abstract—This paper describes measurements and analytical modeling of the indirect coupling of electromagnetic fields produced by horizontal and vertical lightning currents into the Sago mine located near Buckhannon, WV. Two coupling mechanisms were measured: direct and indirect drive. Only the results from the indirect drive and the associated analysis shall be covered in this paper. Indirect coupling results from electromagnetic field propagation through the earth as a result of a cloud-to-ground lightning stroke or a long, low-altitude horizontal current channel from a cloud-to-ground stroke. Unlike direct coupling, indirect coupling does not require metallic conductors in a continuous path from the surface to areas internal to the mine. Results from the indirect coupling measurements and our modeling show that vertical lightning currents are not likely to have produced lethal voltages in the Sago mine, but a large, horizontal current above the ground could have created a large voltage on a long, insulated cable. Indirect transfer function measurements compare extremely well with analytical and numerical models developed for the Sago site, which take into account measured soil and rock overburden properties.

Index Terms—Buried cables, cables, electromagnetic coupling, electromagnetic measurements, lightning, model validation, modeling.

I. INTRODUCTION

ON JANUARY 2, 2006, an explosion was initiated in a methane–air mixture within a sealed area at the Sago underground coal mine near Buckhannon, WV, which resulted in the deaths of 12 miners. Because of the fraction of a second simultaneity of the explosion and nearby lightning strokes recorded by the National Lightning Detection Network (NLDN) and the United States Precision Lightning Network (USPLN), lightning was strongly suspected to have caused the explosion. Additional eyewitness reports of other lightning, not recorded by NLDN and USPLN, further increase these suspicions [1]. Since 1990, at least 11 underground coal mine explosions have

occurred in the U.S. in which lightning is suspected of being the cause, further supporting the need to understand the potential role of lightning in the Sago disaster [2]–[5]. The coupling mechanisms that may have brought lightning energy into the sealed area 300 ft below ground at Sago were unclear and complicated by the fact that there were no known metallic penetrations into the sealed area of the Sago mine, unlike other sealed area explosions.

Recent work by Novak and others [6], [7] have utilized commercial, numerical electromagnetic codes to calculate the voltages on metal-cased boreholes connecting the surface with the sealed areas in mines. They have postulated corona discharge as an initiating mechanism based on experimental work by combustion researchers [8], [9]. Berger *et al.* have analyzed the specific situation of lightning-caused explosions in shallow South African underground coal mines [10]–[14]. The Australian, German, and Chinese literature on lightning-initiated underground coal mine explosions has not been thoroughly explored. There has also been work by Petrache *et al.* [15], [16] on induced voltages on buried cables due to lightning; however, the cables were only buried at a depth of the order of 1 m. Delfino *et al.* [17] also calculated the underground electromagnetic fields due to lightning at depths of 10 m and less.

The coupling mechanisms of lightning energy at the Sago mine were divided into: 1) direct coupling via metallic penetrations from the outside of the mine that are terminated immediately outside the sealed area and 2) indirect coupling through the soil and rock overburden above the sealed area. Direct-drive measurements [18] demonstrate that the direct coupling path was unlikely to have caused the Sago mine explosion. Only the indirect coupling path is discussed in this paper. However, a follow-on paper describing the direct-drive measurements, results, and possible shock safety concerns due to lightning attachment is in preparation.

A. Coupling Transfer Function Measurements and Analysis

Three steps are involved in calculating the response of a lightning flash attachment at a distance from the sealed area. The first step involves estimating the magnetic field (or surface current) above the sealed area from a lightning attachment to the ground at a distance from the sealed area. The second step involves calculating the electric field in the sealed area of the mine due to the uniform magnetic field (or surface current) on the surface using the parameters determined from the coupling measurements. Once these connections are made with data in the frequency domain, the third step is to multiply the Fourier transform of a mathematical representation of a lightning flash by the transfer

Manuscript received June 25, 2008; revised February 28, 2009 and July 30, 2009. First published December 31, 2009; current version published February 18, 2010. This work was supported in part by the Mine Safety and Health Administration. Sandia is a multiprogram laboratory operated by Sandia Corporation, a Lockheed Martin Company, for the U.S. Department of Energy's National Nuclear Security Administration under Contract DE-AC04-94AL85000.

M. B. Higgins and M. Caldwell are with the Electromagnetic Effects Group, Sandia National Laboratories, Albuquerque, NM 87185 USA (e-mail: mbhiggi@sandia.gov; mcaldw@sandia.gov).

M. E. Morris is with the Electromagnetic and Plasma Physics Analysis group, Sandia National Laboratories, Albuquerque, NM 87185 USA (e-mail: memorri@sandia.gov).

C. G. Christodoulou is with the Department of Electrical and Computer Engineering, University of New Mexico, Albuquerque, NM 87131 USA (e-mail: cgc@unm.edu).

Color versions of one or more of the figures in this paper are available online at <http://ieeexplore.ieee.org>.

Digital Object Identifier 10.1109/TEMC.2009.2036928

function derived in the first two steps. The inverse Fourier transform of the product can be taken to determine the peak electric field and peak voltages that would be caused by a lightning attachment of a given amplitude at a given location with respect to the sealed area. If the peak-induced voltages are significant, arcing between conductors could occur. A few tenths of a millijoule of energy in the arc would be a sufficient ignition source for a combustible methane–air mixture [19]. This amount of energy is readily available from almost any arcing process envisioned in a lightning-induced event. Bulk air breakdown in small gaps (several millimeters) occurs at average electric field values of approximately 10 kV/cm with standard lightning waveforms [20]. Surface arcing can occur at electric field values in the 5-kV/cm range.

When a vertical lightning flash attaches to the earth, current travels into the earth, as evident by fulgurites and along a surface layer away from the attachment point. For this paper, we have assumed a fully developed lightning flash and approximated the azimuthal magnetostatic field as

$$H(r) = \frac{I}{2\pi r} \quad (1)$$

where I is the lightning current and r is radial distance from flash attachment. This approximation is valid for distances where $r \ll h_0$, where h_0 is the height of the charge source [21]. The electric and magnetic fields near rocket-triggered lightning have been measured, and the current flow in the soil out to 30 m distance from the attachment can be inferred [22], [23]. When $r \gg h_0$, the vertical component of the electric field can be approximated using

$$E_z^{\text{rad}}(r, t) = \left[\frac{-v}{2\pi\epsilon_0 c^2 r} \right] I(0, t - r/c) \quad (2)$$

where v is the upward propagation speed of the current wave and is the same as the front speed in many engineering models [21], [24]. For distances where r is not much less or much greater than h_0 , the approximation for the magnetic field at the surface becomes more complex, as shown by Thottappillil *et al.* [25]. Calculated field results from Nucci *et al.* [26] at a distance of 5 km show peak values of 0.265 A/m. These results can be bounded by using (1), which yields 0.35 A/m for $I = 11$ kA. Therefore, using (1) at 1–5 km is an overestimation of the field, but can be used as a simple approximation.

When lightning attaches to the ground, the azimuthal magnetic field creates currents not only on the surface, but also deeper in the earth. This is because magnetic fields on the surface of a conductor can generate currents within a conductor of some depth. Resistivity measurements have shown the soil in the vicinity of the sealed area of the Sago mine to be a fairly good conductor; therefore, it is reasonable to assume that some electromagnetic energy can propagate from the surface of the earth through the overburden into the sealed area of the mine. The electromagnetic coupling is dominated by diffusion coupling when frequencies are sufficiently low that the displacement currents are negligible. Diffusion coupling is also referred to as eddy current coupling. The skin depth characterizes the

exponential decay of these currents in planar geometries and is dependent on the resistivity of the soil.

It was desired to measure the coupling through the earth into the sealed area due to a realistic lightning strike. Because of safety and time considerations, inducing a lightning strike or waiting for a real one were not viable options. Therefore, a low-power, frequency-variable source was used to drive current on long wires on the surface. The wires were 200–500 m long and terminated with ground rods. An antenna was used to measure the resulting electric field in the sealed area, 300 ft below the drive wires on the surface. In addition, voltage induced on a long, insulated pump cable abandoned in the sealed area was also measured. Measurement setup details are given in Section III.

The frequency range of the source was chosen to match the frequency content of a realistic lightning strike. Long wires were used to simulate current traveling radially on the surface from lightning attaching to the surface. They realize that there were multiple limitations to this approach and conducted modeling in tandem to test the validity of this approach. One limitation was that the range of the frequency-variable source was 10 Hz–100 kHz, while realistic lightning has frequency content up to a few megahertz. Another concern was that the source-driving long wires on the surface was not a sufficient representation of lightning traveling radially on the surface from an attached lightning strike. Another concern was that unknown resistive inhomogeneities in the soil and rock above the sealed area could affect the results. Despite these concerns, the modeling and measured results compared favorably, as can be seen further in this paper. This does not invalidate these concerns, but does lend credence to the deduction that they were not overwhelmingly important factors in this case.

From the measurements, we have the electric field and voltage response on the pump cable in the sealed area from a known linear current distribution on the surface.

B. Site Information

The soil and rock resistivities play a major role in determining the amplitude and frequency dependence of indirect coupling into the sealed mine area. The resistivities in [27], using a best fit to electromagnetic sounding data, are 100 $\Omega\cdot\text{m}$ from 0 to 40 ft, 10 $\Omega\cdot\text{m}$ from 40 to 120 ft, and 100 $\Omega\cdot\text{m}$ from 120 to 350 ft deep, yielding an average of 77.3 $\Omega\cdot\text{m}$ above the sealed area at the borehole. In this study, an average resistivity of 80 $\Omega\cdot\text{m}$ is used to characterize the soil and rock overburden above the sealed area of the Sago mine.

Vertical pipes, including gas wells, in the vicinity of the sealed area, are potential conduits for lightning energy. Because the pump cable in the sealed area is orthogonal to the pipes, the vertical pipes were considered not to be a likely source of significant coupling to the cable in this particular case and were not investigated.

There were also horizontal gas pipes in the vicinity above the sealed area. This includes approximately 27 mi of horizontal (mostly metal) gas pipelines within 1.5 mi of the Sago explosion area, and these pipes are connected to 60 active gas wells

(going to an average depth of 3800 ft). These horizontal pipes are, in general, buried at a depth of 2 ft from the surface. The response on the pump cable, or electric fields in the sealed area, due to the current drive of the horizontal gas pipes was not characterized because it was not planned for and because of liability issues that could not be resolved in the short time frame of the planned measurements. The gas pipes, if driven locally to the sealed area, would have similar coupling characteristics to the pump cable as that of the indirect-drive experimental setup. If the gas pipes were driven remotely, the amount of attenuation from one point on the pipes to another point is mostly dependent upon the resistivity of the soil surrounding the pipes. If the soil surrounding the pipes has low resistivity, a majority of current injected onto the pipes would attenuate in a short distance. However, if the pipes are either not in contact with the soil or the resistivity of the soil is large, then the pipes would act as insulated conductors. Attenuation along the pipes in this case would be much less.

C. Outline of Paper

Section II presents the derivation of the models used to predict the coupling of surface current to underground electric fields. The geometry for the simplest model for dc current coupling is analyzed in [28]. The discussion in this paper bypasses the simple static representation of the problem and begins with a time-varying infinite current drive above the surface. The equation can be simplified when the current is brought to the surface interface. Section III presents the measurement techniques, including diagrams of the setup and photos graph of equipment. Section IV presents the measured data and a comparison with the model from Section II. Conclusions are presented in Section V.

II. ELECTROMAGNETIC COUPLING PHENOMENOLOGY MODELS

Modeling was included in this project to compare the measurements with theoretical calculations. Another purpose of the indirect modeling was to determine if the simple propagation models from surface to underground were sufficient for these lightning propagation calculations.

This section documents the relevant analytical models used to predict the voltages and electric fields produced in the Sago mine by current drive sources used to simulate the effects of a lightning flash attachment on the surface of the earth above the mine. To calculate the electric fields in the earth induced by a current on the surface, the problem is simplified by representing the earth as a homogeneous material with a constant uniform resistivity. Section II-A calculates the simplest case given an infinite-length, time-varying current drive. The calculations become less complex in Section II-B as the current drive is brought to the surface. These results are used to compare to the indirect measurements of the electric field in the sealed area as a function of the drive current on the surface. The modeling equations have been implemented in MATLAB to calculate the fields and the resulting voltages generated within the earth.

It should be noted that Rakov and Uman [29] and Cooray [30] have developed equations for calculating the aboveground and underground electric field from a lightning return stroke. The

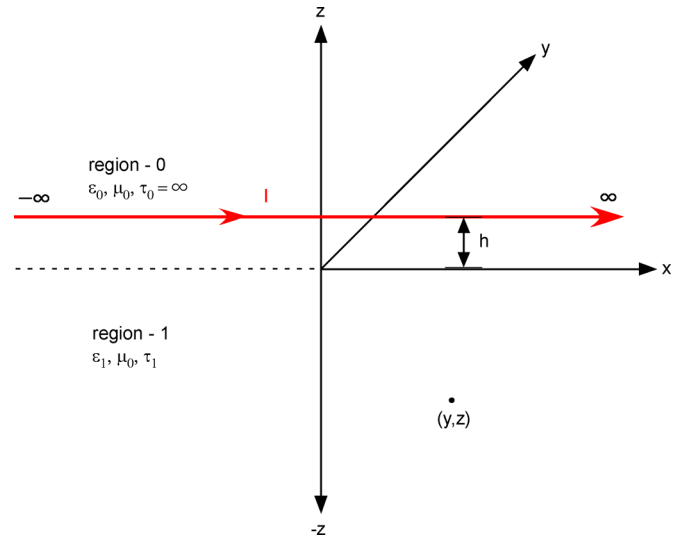


Fig. 1. Infinite length, harmonically time-varying horizontal current drive over a conductive half-space.

electric fields calculated from the simple method described in this paper were compared to the results in [30] and were found to be within 10% of peak values.

A. Infinite Line Source Above Homogeneous Half-Space

The first coupling models to be considered are generalizations, where the current is time varying, say as with $e^{i\omega t}$, and the displacement currents are neglected because region 1 is assumed to be a good conductor. This generalization turns out to be more difficult than one might expect because the current in the earth depends on the geometry of the current path above the earth. A simpler model that corresponds to the electromagnetic coupling below an infinitely long, horizontal wire grounded at a large distance away and driven by a voltage source is, however, developed in this section.

The current drive geometry of an infinitely long, horizontal wire placed a distance h above a conductive half-space is shown in Fig. 1. Similar configurations are analyzed in [31]–[35].

The current drive is harmonically time varying and directed along the x -axis at height h above it. The upper half-space has permittivity ϵ_0 and infinite resistivity, and the lower half-space has permittivity ϵ_1 and resistivity τ_1 . Both regions have free space permeability μ_0 .

If one neglects displacement current and relates current density $i_x(y, z)$ and electric field $E_x(y, z)$ in region-1 through $E_x(y, z) = \tau_1 i_x(y, z)$, then the current density in the lower half-space, region-1, can be determined to be

$$\begin{aligned} i_x(y, z) &= -\frac{i\omega\mu_0 I}{\pi\tau_1} \int_0^\infty \frac{e^{qz} e^{-uh}}{u+q} \cos uy \, du \\ &= \frac{i2}{\pi} \frac{I}{\delta_1^2} \int_0^\infty \frac{e^{qz} e^{-uh}}{u+q} \cos uy \, du \end{aligned} \quad (3)$$

and then

$$E_x(y, z) = \tau_1 i_x(y, z) = \frac{ik\zeta_0}{\pi} \int_0^\infty \frac{e^{qz} e^{-uh}}{u+q} \cos uy \, du \quad (4)$$

where

$$\begin{aligned} k &= \omega \sqrt{\mu_0 \varepsilon_0} \\ q &= \sqrt{u^2 + ip^2} \\ p^2 &= \frac{\omega \mu_0}{\tau_1} = \frac{2}{\delta_1^2} \\ \delta_1 &= \sqrt{\frac{2\tau_1}{\omega \mu_0}}. \end{aligned}$$

Note that the skin depth δ plays an important role as a parameter in all diffusion coupling calculations. At a given frequency, the lower the resistivity the smaller the skin depth, which means that a majority of the current is contained closer to the surface. Hence, for a given surface magnetic field drive, there will be better coupling deeper underground for ground with resistivity of 100 $\Omega \cdot \text{m}$ than for ground with resistivity of 10 $\Omega \cdot \text{m}$.

B. Infinite Line Source at Surface of Homogeneous Half-Space

If the line current source is brought to the surface of the conducting homogeneous half-space where $h = 0$, integrating E_x from the previous section for $y = 0$ to get the horizontal electric field immediately below the current source yields [18]

$$E_x(y=0, z) = \frac{\tau_1 I}{\pi \delta_1^2} \left\{ \begin{array}{l} \left[(1+i) \frac{1}{\left(\frac{z}{\delta_1}\right)} + \frac{1}{\left(\frac{z}{\delta_1}\right)^2} \right] e^{-(1+i)(z/\delta_1)} \\ -i2K_0 \left[(1+i) \frac{z}{\delta_1} \right] \\ -(1+i) \frac{1}{\left(\frac{z}{\delta_1}\right)} K_1 \left[(1+i) \frac{z}{\delta_1} \right] \end{array} \right\} \quad (5)$$

where K_0 and K_1 are modified Bessel functions. Note that we are now using positive z in the downward direction in the formula.

C. Finite Line Source at Surface of Homogeneous Half-Space

The time-harmonic fields underground due to a finite line current have been studied by Hill and Wait [36]. Again, displacement currents are neglected due to the low frequency of interest. The field components calculated are as follows:

$$\begin{aligned} E_x(x, y, z) &= \frac{-I}{2\pi\sigma} \int_{-l}^l (A+B) \, dx' \\ A &= \frac{\exp(-\gamma r)}{r^3} \left[\left(\frac{3z^2}{r^2} - 1 \right) + \gamma r \left(\frac{3z^2}{r^2} - 1 \right) + \gamma^2 z^2 \right] \end{aligned}$$

$$B = \frac{\gamma}{2} \left[\begin{array}{l} \frac{\gamma z}{r^2} \left(1 - \frac{3y^2}{r^2} \right) I_0 K_0 + \frac{\gamma z}{r^2} \left(-1 + \frac{3y^2}{r^2} + \frac{2y^2}{r^2 - z^2} \right) I_1 K_1 \\ + \frac{1}{r^2} \left(-1 + \frac{3y^2}{r^2} + \frac{z(1-\gamma^2 y^2)}{r} - \frac{3zy^2}{r^3} \right) I_0 K_1 \\ + \frac{1}{r^2} \left(-1 + \frac{3y^2}{r^2} - \frac{z(1-\gamma^2 y^2)}{r} + \frac{3zy^2}{r^3} \right) I_1 K_0 \end{array} \right]. \quad (6)$$

The argument of I_0 and I_1 is $\gamma(r+z)/2$, and the argument of K_0 and K_1 is $\gamma(r-z)/2$.

D. Transmission-Line Field Coupling Model

Using transmission-line theory and treating the incident electric field as a distributed source, has been used in previous areas by Vance [37] and Warne and Chen [38]. We consider the receiving wire in the mine as a wire over a lossy earth ground, where the radius of the wire is a and the wire is at distance d above the ground. Then, we let

$$k = \sqrt{-ZY} \text{ and } Z_c = \sqrt{\frac{Z}{Y}}. \quad (7)$$

For the admittance, we use the usual formulation of a wire over a perfect ground for the capacitance, such that

$$Y = i\omega C = \frac{-i\omega 2\pi\varepsilon_0}{\text{arccosh}(d/a)}. \quad (8)$$

For the impedance, the perturbation due to the nonperfect ground is included using Sunde's formulation [39], [40] $Z = Z_1 + Z_2$, where Z_1 is the formulation of a wire over a perfect ground and Z_2 is the correction term, which are as follows:

$$\begin{aligned} Z_1 &= \frac{-i\omega\mu_0 \text{arccosh}(d/a)}{2\pi} \\ Z_2 &= \frac{-i\omega\mu_0 \Delta}{2\pi} \end{aligned} \quad (9)$$

where $\Delta = \ln(1 - idk_d / -idk_d)$ and $k_d = \sqrt{\omega\mu_0(i\sigma_d + \omega\varepsilon_d)}$.

Then, the transmission-line equations start as

$$\begin{aligned} \frac{dV^s}{dx} &= -ZI + E_x^{\text{inc}} \\ \frac{dI}{dx} &= -YV^s \end{aligned} \quad (10)$$

where V^s is the scattered voltage and the total voltage V is described as

$$V(x) = V^s(x) - \int_0^h E_z^{\text{inc}}(x, z) \, dz. \quad (11)$$

Letting $h = 0.01$ m for an insulated cable on the ground allows for $V(x) \sim V^s(x)$. Also, V is the total voltage if the vertical component of electric field in the absence of the cable is equal to zero [41].

Combining (10) by differentiating (second equation) yields

$$\left(\frac{d^2}{dx^2} + k^2\right) I = -Y E_x^{\text{inc}}. \quad (12)$$

If we let E_x be a constant, then solving the second-order differential equation yields

$$I(x) = \frac{-E_x^{\text{inc}}}{Z} (\tan(kL) \sin(kx) + \cos(kx) - 1). \quad (13)$$

Also, at $x = 0$ (where the measurements were made)

$$V(0) = \frac{k E_x^{\text{inc}}}{YZ} \tan(kL). \quad (14)$$

If E_x is allowed to be a function of x , then using the method of variation of parameters, we find

$$I(x) = (C_1 + P(x)) e^{-kx} + (C_2 + Q(x)) e^{kx} \quad (15)$$

where

$$\begin{aligned} P(x) &= \frac{1}{2Z_c} \int_{x_1}^x e^{kv} E_x^{\text{inc}}(v) dv \\ Q(x) &= \frac{1}{2Z_c} \int_x^{x_2} e^{-kv} E_x^{\text{inc}}(v) dv \\ C_1 &= \rho_1 e^{kx_1} \frac{\rho_2 P(x_2) e^{-kx_2} - Q(x_1) e^{kx_2}}{e^{k(x_2-x_1)} - \rho_1 \rho_2 e^{-k(x_2-x_1)}} \\ C_2 &= \rho_2 e^{-kx_2} \frac{\rho_1 Q(x_1) e^{kx_1} - P(x_2) e^{-kx_1}}{e^{k(x_2-x_1)} - \rho_1 \rho_2 e^{-k(x_2-x_1)}} \\ \rho_1 &= \frac{Z_1 - Z_c}{Z_1 + Z_c} \text{ and } \rho_2 = \frac{Z_2 - Z_c}{Z_2 + Z_c}. \end{aligned} \quad (16)$$

The impedance at x_1 ($x = 0$) is set to be 10 M Ω , which is essentially an open circuit, and the impedance at x_2 ($x = 300$ m) is set to be 0, or a short-circuit. These conditions lead to $P(x_1)$ and $Q(x_2)$ equal to zero, ρ_1 equal to 1, and ρ_2 equal to -1 . The voltage at x_1 is

$$V(x_1) = Z_c \left(\frac{-Q(x_1) \sinh(kx_2) - P(x_2) e^{-kx_2}}{\cosh(kx_2)} - Q(x_1) \right). \quad (17)$$

E. Uniform Magnetic Field at Surface Above Homogeneous Half-Space

The fields produced in the sealed area during the explosion were from natural lightning, not linear current sources. In Section I-A, the magnetic field from a fully developed vertical lightning flash was shown. This magnetic field can be calculated at a distance on the surface from the flash attachment point, but we still need to propagate the field to the sealed area below the surface. This section develops the equations that allow a uniform magnetic field to propagate into a conductive half-space and calculate the electric field in the half-space. The results of this derivation are identical to [42, eq. (1)] and [43, eq. (6)].

Assume that a uniform y -directed magnetic field of intensity H_0 is instantaneously applied above a conducting half-space.

For a good conductor [44]

$$\begin{aligned} \alpha &\approx \sqrt{\frac{\omega \mu \sigma}{2}} = \frac{1}{\delta} \\ \beta &\approx \sqrt{\frac{\omega \mu \sigma}{2}} = \frac{1}{\delta}. \end{aligned} \quad (18)$$

The surface impedance is written as

$$Z_S = (1 + i) \sqrt{\frac{\omega \mu_1}{2\sigma_1}}. \quad (19)$$

Taking the normal unit vector to be in the z -direction and applying the boundary condition of surface impedance, yields the tangential electric field as

$$\vec{E}_t = Z_S \vec{J}_S = Z_S (\hat{n} \times \vec{H}) = -\hat{x} Z_S H_{0y}. \quad (20)$$

Substituting the formula for the surface impedance and skin depth, and rearranging yields the electric field just below the surface of the interface

$$\begin{aligned} E_{1x}(z = 0^-) &= -(1 + i) \sqrt{\frac{\omega \mu_1}{2\sigma_1}} H_{0y} \\ &= -(1 + i) \frac{1}{\sigma_1} \frac{1}{\delta_1} H_{0y} \\ &= -\tau_1 \frac{(1 + i)}{\delta_1} H_{0y}. \end{aligned} \quad (21)$$

However, it is more important to know the electric field below the surface at some depth $z = -d$. Therefore, for attenuation in the negative z -direction

$$E_{x1}(z) = E(z = 0^-) e^{(\alpha + i\beta)z}. \quad (22)$$

Combining the previous equations yields the x component of the electric field due to a uniform magnetic field at the surface as

$$E_{x1}(z) = -\tau_1 \frac{(1 + i)}{\delta_1} H_{0y} e^{(1+i)z/\delta_1}. \quad (23)$$

III. ELECTROMAGNETIC MEASUREMENT METHODS

The measurement method used to characterize indirect electromagnetic coupling into the sealed area is shown in Figs. 2 and 3. The current from an audio amplifier (which is driven by the output from a network analyzer) is driven on long wires above the ground, which are terminated at each end with ground rods. The ground rods are placed so that the drive wire was in a straight line, to produce a current distribution in the ground that simulates a linear current drive.

Two orthogonal drive cable orientations were used for the indirect-drive measurements. One orientation, shown in Fig. 3, drove the surface current parallel to the sealed area of the mine and over the area where the explosion occurred. The surface drive wire was approximately 500 m long. The second orientation, not shown, drove the surface current perpendicular to the sealed area of the mine and over the area where the explosion occurred. In this case, the surface drive wire was only 200 m long. Using the results from these two configurations, the fields due to an arbitrarily oriented current source drive above

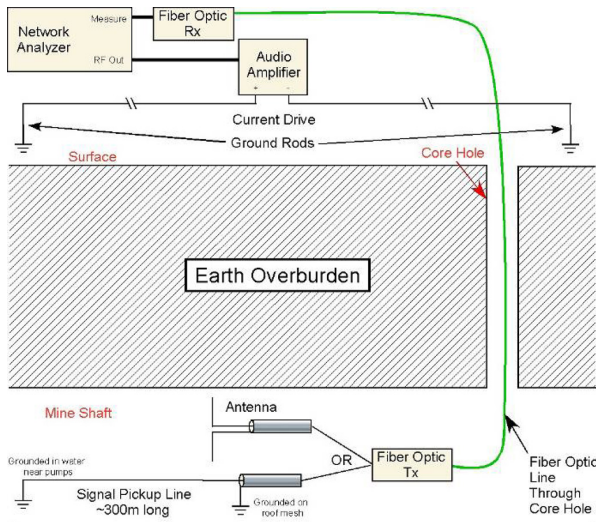


Fig. 2. Indirect-drive conceptual drawing.

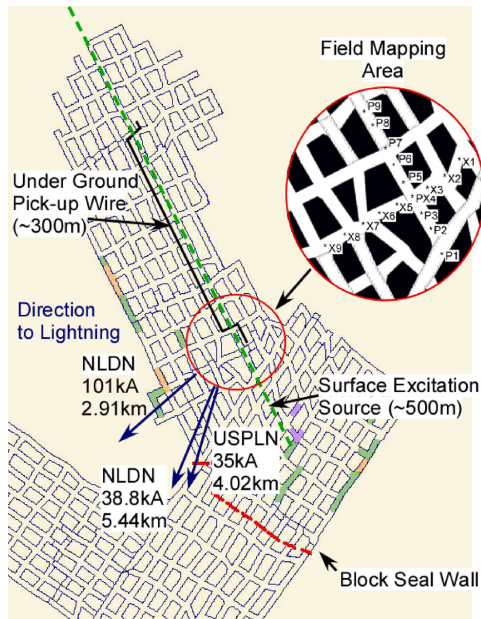


Fig. 3. Parallel surface current drive for the indirect-drive measurements with electric field measurement locations.

the sealed area can be calculated using trigonometric functions, thus accounting for all angles of current source orientation.

The measurement method developed utilizes the dynamic range and frequency sweep speed of a network analyzer. In addition, the transfer function has both amplitude and phase information, which is important to ensure causality in an inverse Fourier transform. The key to the method is the use of a fiber-optic transmitter/receiver pair with an operational frequency band from dc to ~ 10 MHz. The fiber-optic units were used to bring the measured signals from the sealed area to the surface through a nonconductive borehole. It would increase the dynamic range of the measurement system to place the fiber optics on the drive side; however, transporting the network analyzer deep into the previously sealed area was an unattractive

alternative. Therefore, a reduction in dynamic range was traded for speed of equipment setup and a reduced risk of damaging expensive equipment. The audio amplifier, with an output impedance of $4\ \Omega$, matched the impedance of the grounded wire drives sufficiently well to generate enough surface current to measure signals in the sealed area below. The frequency range of the audio amplifier was 10 Hz–100 kHz. Communication between team members on the surface and members positioned in the previously sealed area of the mine was accomplished using a fiber optic Ethernet link through the borehole with a voice over IP program on two laptops.

Two types of measurements were made to characterize the indirect coupling into the sealed area. The more time consuming of the two was the electric field mapping measurements made in the vicinity of the explosion ignition area, where the core hole is located. The other measurement was the induced voltage on a pump cable going from the back of the sealed area to the location of the core hole.

The electric field at various locations in the sealed area of the mine was measured with an active dipole antenna connected to a receiver via fiber optics. The fiber-optic receiver was connected to the network analyzer measurement port so that the signals were phase-locked in order to measure very small signals in the microVolt/meter range. The three polarizations of the electric field were measured at a total of 15 locations for both the parallel and perpendicular surface wire current drives. The three polarizations measured were the vertical polarization, the horizontal P -directed polarization (parallel to the length of the sealed area), and the horizontal X -directed polarization (transverse to the length of the sealed area). A photo graph of the dipole antenna in one of the horizontal polarizations is shown in Fig. 4. The measured calibration frequency response of the active dipole antenna is shown in Fig. 5. The exact locations of the measured electric field are shown in Fig. 3, where the distance between measurement locations was approximately 10 m. The figure shows 17 total locations; however, positions P1 and P9 were not measured due to water hazards. In other words, there were seven locations where the electric field was measured (parallel to the underground wire orientation) and these points were spaced approximately 10 m apart. Because of the amount of data taken and the spacing between measurement points, the lack of these two points did not negatively impact the results.

The pump cable was spliced with 12-gauge wire to recreate the length of pump cable believed to have been there during the explosion.¹ The end of the pump cable at the back of the mine was originally attached to the pump that was submerged underwater and chained to the ceiling mesh. For the measurements, the pump cable was connected with 12-gauge wire to the ceiling mesh and the exposed conductors were placed underwater approximately four crosscuts from the back of the sealed area.² The cable being attached to the ceiling mesh on one end grounds

¹As a note, there is some disagreement as to the length and positioning of the pump cable at the time of the explosion. The test team used information provided at the time of the measurements, which was that the pump cable was intact and the cable shield was grounded to the submerged pump.

²Test team was unable to reach the back of the sealed area, where the pump would have been (it was removed after the explosion) due to water.



Fig. 4. Active dipole antenna in the horizontal polarization inside the previously sealed area.

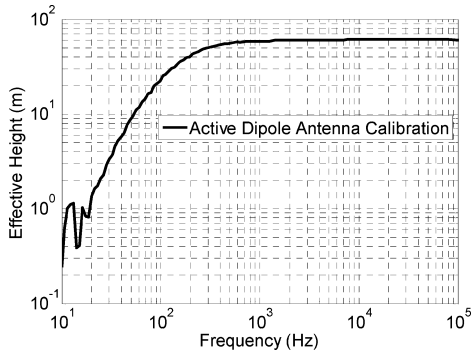


Fig. 5. Calibration frequency response of active dipole antenna.

that end of the cable through the roof mesh. The approximate total length of the recreated cable was 300 m. The induced voltage measurements were taken on the pump cable with both a parallel and perpendicular surface wire drives. These measurements were also conducted using the instrumentation system shown in Fig. 2. The induced cable voltage was measured with a Nanofast high-impedance probe in the vicinity of the core hole, and transmitted to the surface with fiber optics.

IV. RESULTS

The purpose of the electric field mapping of the explosion area was to first look for any field inhomogeneities due to geological features and second, to compare to the analytical model. The electric field measurements are shown first and then the induced cable voltage is plotted. The results did show an enhanced electric field at the P5 location. This is noted for general interest, but does not significantly impact the cable results because the

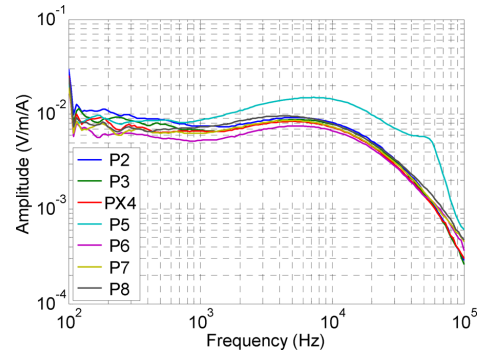


Fig. 6. Composite electric field along the P -direction with parallel line drive on surface.

cable integrates or averages the fields over the cable length to build up a potential difference or voltage.

The data collected for the indirect-drive tests from the dipole antenna were only usable above 100 Hz. This was due to a very large 60-Hz clutter signal from surrounding power lines and the high noise level from the network analyzer below 40 Hz. Both of these factors were overcome for the long wire voltage measurement by reducing the IF bandwidth of the network analyzer from 10 to 2 Hz. The reduction of the IF bandwidth lowered the noise floor considerably and reduced the sensitivity of the transfer function to the 60 Hz clutter; however, the time for a single swept measurement increased by almost a factor of 10. With the large number of measurements desired for characterizing the electric field in the sealed area, the higher IF bandwidth was used for the majority of the data collected. As a result, only data from frequencies above 100 Hz are plotted in Fig. 6.

The normalized composite electric fields from the dipole antenna at various locations are plotted in this section. The composite electric field is simply the root-sum-square or amplitude of the electric field vector. The measured electric field is normalized by the current in the drive wire on the surface, so that the units are volts per meter per ampere [V/(m·A)].

The normalized electric fields due to the wire current drive parallel to the P -direction, measured at locations P2 through P8, are shown in Fig. 6.

Referring to Fig. 6, note that all composite electric fields measured in a path parallel to and immediately below the drive are approximately the same amplitude. The measurement at P5 was made in the area between unconnected sections of roof mesh and shows a slight enhancement. The presence of metal objects near an antenna can affect the local fields. The slight resonance at about 60 kHz in the P5 measurement was probably caused by a resonance of the cable that was attached for the voltage measurements. This cable was not removed for the electric field measurements, and high electric fields may have been induced on the disconnected end of the cable at resonance.

The voltage on the pump cable was measured with a high-impedance voltage probe and the network analyzer set to a 2-Hz IF bandwidth. The normalized results of the voltage amplitude plotted relative to the drive current on the surface wire, with units of volts per ampere (V/A), are shown in Fig. 9.

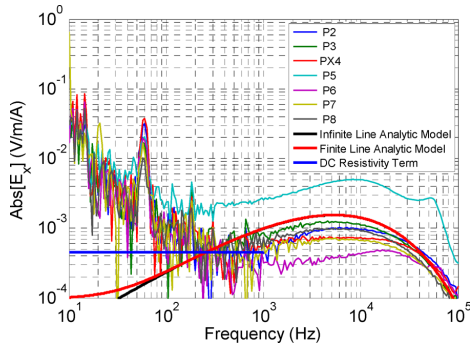


Fig. 7. P -directed electric fields compared with the analytic models with an effective resistivity of $80 \Omega \cdot \text{m}$.

To compare the induced voltage measured on the pump cable with the field measurements, we will look only at the parallel surface-drive-induced fields from P2 to P8. Furthermore, we will only look at the horizontal polarization directed along the P -axis, parallel to the direction of the drift. The horizontal polarized electric fields are shown in Fig. 7. The normalized electric fields are in units of volts per meter per ampere, while the normalized induced voltages on the pump cable is in units of volts per ampere. The distributed source transmission-line model is used for coupling the electric field onto the cable in the following section.

A. Results Compared With Diffusion Model

The model for coupling from an infinite and a finite current source above a homogeneous half-space were presented in Section II. These models are compared with the measured electric field. Using an effective soil resistivity of $80 \Omega \cdot \text{m}$, the analytic models plotted in Fig. 7 match very closely to the horizontal (P -directed) electric field measured with a parallel current drive. The correlation between model and measured data is extremely good from below 1 to 100 kHz. This confirms that the major coupling mechanism from the surface to the sealed area is field diffusion coupling. The measured data are contaminated by 60-Hz resonances and clutter below 1 kHz for this polarization. The data deviate from the model of coupling beneath an infinite line at frequencies below 1 kHz. The measured data stay at a constant level of approximately 0.0006 V/m/A , whereas the analytical model predicts a downward slope. Much of this deviation can be attributed to the field caused by the dc component from the finite spacing of the ground rods. The numerical simulations in Electromagnetic Interactions GEneralized (EIGER), a frequency-domain electromagnetics code, account for the low-frequency enhancements due to the finite length of the cable much better than the analytic models. A comparison of the average of the P -directed electric field measurements from P2 to P8 with the analytic models and the numerical models is shown in Fig. 8. The average field is a more meaningful value to compare since it has local variations removed. The amplitude and shape show amazing correlation.

To compare the numerical model with the measured induced cable voltage, we used a distributed source transmission-line

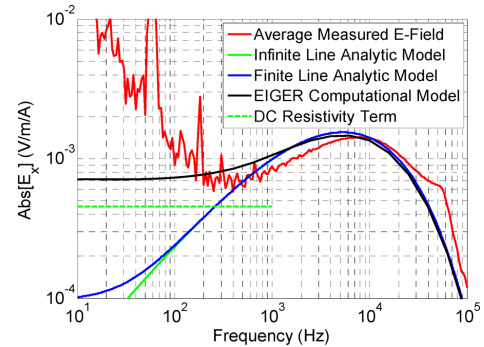


Fig. 8. Average of the P -directed fields from P2 to P8 compared with analytic and numerical models.

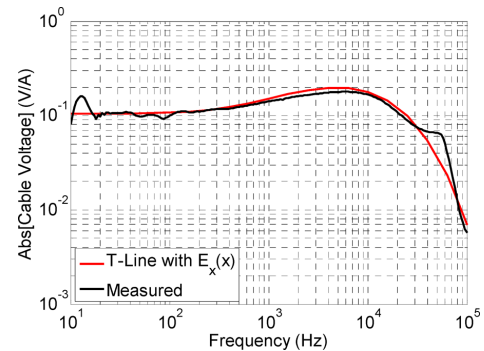


Fig. 9. Induced voltage on the pump cable due to parallel wire current drive on the surface (with 60 Hz and harmonics removed) compared with distributed transmission line coupling from the numerically calculated electric field and an effective soil resistivity of $80 \Omega \cdot \text{m}$.

model for coupling. Again, the model shows excellent agreement with the measured voltage through the entire range of frequencies. The measured data have been processed to remove the 60-Hz clutter signal and its harmonics as shown in Fig. 9.

B. Results Coupled With Lightning Waveforms

The results from the indirect coupling measurements and analysis are coupled with recorded and hypothetical lightning strokes in this section. The hypothetical strokes were assumed to have a peak amplitude of 100 kA for two reasons: first, there was a cloud-to-ground stroke recorded close in time and distance to the explosion area of the order of 100 kA; and second, the value of 100 kA is easy to scale. It should be noted that the pump cable voltages for the recorded strokes were calculated using the uniform magnetic field excitation formulation shown in Section II-E. The voltages from a hypothetical long, low-altitude horizontal current channel from a cloud-to-ground stroke were calculated using infinite line current source above a half-space shown in Section II-A. The basic lightning waveforms used in this section as inputs into the transfer functions are shown in Fig. 10. No analytic or mathematical model for a positive lightning waveform was found in published literature. Hence, a positive lightning waveform was created using a 15th-order polynomial of the author's design and appending a 100-ms tail on the backend. The positive lightning waveform characteristics were tailored from values found in [45] and [46].

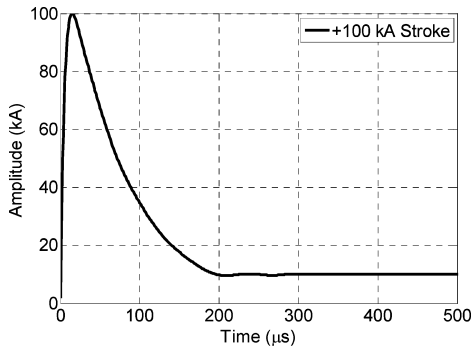


Fig. 10. Modeled 100-kA positive lightning stroke with a dI/dt of $6.5 \text{ kA}/\mu\text{s}$ and a full-width half maximum of $69 \mu\text{s}$.

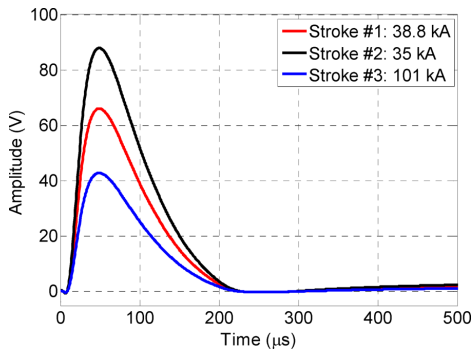


Fig. 11. Voltage induced on pump cable due to the three positive lightning strokes recorded on the NLDN and USPLN.

The three closest lightning strokes recorded within 1 s of the Sago explosion by the NLDN and USPLN were used to calculate voltage induced on the pump cable. The angles discussed are the angle between the line made up from the lightning stroke location to the center of the pump cable and the line formed by the direction where the pump cable lay. The first stroke analyzed is the 38.8-kA positive lightning stroke, 5.44 km away from the sealed area, and an angle of 52.8° . The second stroke has an amplitude of 35 kA at a distance of 4.02 km away from the sealed area and an angle of 49.3° . (Note that it is highly probable that the 38.8 and 35 kA strokes represent a single stroke with a location discrepancy, as discussed in [18].) The last stroke has an amplitude of 101 kA, a distance of 2.91 km, and an angle of 85.5° . The resulting induced voltage pulses on the pump cable (at the end of the cable nearest the explosion area) are shown in Fig. 11, with peak amplitudes of 66.1, 87.9, and 42.8 V for the three strokes, respectively. The transmission-line coupling model was used for coupling the electric field to voltage on the pump cable in Fig. 11 with a cable length of 300 m. None of the induced voltages from these recorded strokes have the necessary amplitude to cause an arc inside the sealed area.

If we assume a 100-kA positive cloud-to-ground stroke with a long, low-altitude horizontal current channel directly over the sealed area and parallel with the pump cable (a zero-degree angle), it could be capable of inducing voltages on the pump cable sufficient to produce electrical arcing. Pump cable (with a length of 300 m) voltages are shown for a positive cloud-to-ground stroke with horizontal current channel at heights (H)

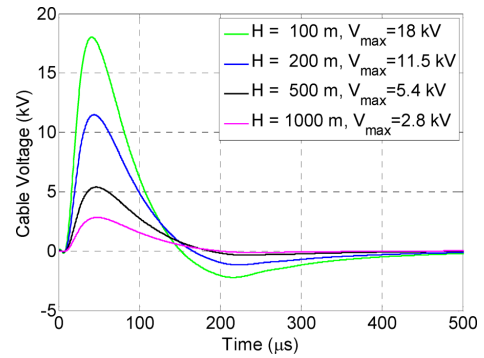


Fig. 12. Induced voltage pulse on pump cable from hypothetical horizontal current channel from a cloud-to-ground +100-kA stroke. H is distance of the current channel above the ground.

of 100, 200, 500, and 1000 m above the surface in Fig. 12. The maximum voltages from the positive current channel at the heights given are 18.0, 11.5, 5.4, and 2.8 kV, respectively.

An eight-layer case based upon the resistivity profile shown in [1] was modeled and yielded peak voltage on the cable 15% less than that of the homogeneous model.

V. CONCLUSION

The results of this short-term project demonstrate the usefulness of transfer function measurement techniques and analytical modeling to evaluate lightning effects in mining environments. Simple analytic and numerical models for coupling electromagnetic energy underground were developed for lightning coupling into the Sago mine. The measured results at the site compared very well with the analytic and numerical models. This study shows that significant field levels and voltages on insulated conductors can be developed from surface current excitations or from overhead lightning arc channels.

Three cloud-to-ground lightning strokes were recorded in the vicinity of the Sago mine within 1 s of the explosion in the sealed area. Based on the results in this paper, these lightning strokes were too far away to have generated a significant voltage on the pump cable in the sealed area. A thorough, expert analysis of the raw data provided by several lightning-detection databases did not uncover evidence to support the detection of another cloud-to-ground stroke in the correct timeframe.

The simultaneous events of recorded lightning strokes and the explosion in the sealed area of the mine; the multiple personal accounts above the sealed area describing simultaneous flash and thunder [1] (indicating extremely close lightning); and the inability of the lightning-detection networks to resolve the presence of horizontal lightning arc channels [45], [46] led to the investigation of a hypothetical lightning stroke event. The expected voltage on the abandoned cable was calculated for this scenario using the indirect coupling models discussed in this paper.

The hypothetical case explored the possibility of the presence of a horizontal lightning arc channel acting as a source of energy. For this scenario, a 100-kA peak horizontal arc channel is assumed to be parallel to the pump cable in the sealed area at distances of 100, 200, 500, and 1000 m, respectively, above the

ground above the sealed area. For a positive-polarity flash, the resultant voltages on the pump cable were 18.0, 11.5, 5.4, and 2.8 kV, respectively. While these calculations use favorable coupling circumstances (high peak arc-channel current and parallel orientation of the arc channel to the pump cable), this hypothetical scenario presents a reasonable case where significant voltages build up on the pump cable.

In conclusion, indirect coupling of lightning of sufficient magnitude and proximity to the sealed area could have created high voltage on the pump cable. The voltages would have been high enough to create an arc, which is a known ignition source of combustible methane–air mixtures. This conclusion is based on the analysis of a hypothetical scenario that is credible and has supporting circumstantial evidence, but could not be confirmed by recorded data from lightning-detection networks.

Due to the complexity of lightning interactions with large multipath structures and the limited duration of this project, it was not possible to address the full intricacies of potential lightning interactions at the Sago mine. However, results cited in this paper can be considered as a significant indicator of the potential for lightning to couple significant voltages to ground on cabling left in underground mines. Significant follow-on research would be required to address the complexity of mining structures to fully characterize these energy-coupling mechanisms.

ACKNOWLEDGMENT

A complex project of this type could not have been undertaken without the funding, coordination, and hard work of the Mine's Safety and Health Administration (MSHA) staff that were involved. The authors would like to thank MSHA staff W. Helfrich, R. Gates, R. Phillips, H. Newcomb, R. Dresch, D. Skorski, J. O'Donnell, and A. Wooten for their support of this project and the ICG staff, C. Dunbar, A. Schoonover, J. Stemple, L. Dean, K. Melvin, and B. Bolyard, for their generous help in arranging access and for providing the services we needed to accomplish the measurement tasks. In spite of our obvious interruptions to their operations as well as extensive demands on their time, they generously provided the services we needed in a timely manner. They would also like to thank the consultants, Dr. T. Novak, Dr. E. P. Krider, E. Checca, and Dr. M. Uman for freely sharing their thoughts on this project. M. Hieb and J. Scott of the State of WV Office of Miners' Health, Safety, and Training provided additional useful information and help to accomplish the work; the property owners of the land above the sealed area, G. Gooden, T. Leggett, B. Patterson, and G. Roessing, for generously allowing us access to their property in order to drive ground rods, string wires, and operate our equipment despite obvious interruptions to their lives; and also their measurement team, D. Charley and L. Martinez, for their extraordinary work in the field. Without their hard work and long hours, the measurements could not have been completed.

REFERENCES

- [1] West Virginia Office of Miners' Health, Safety, and Training. (2006, 11 Dec.). Report of investigation into the Sago mine explosion which occurred January 2, 2006. Upshur Co., Buckhannon, WV. [Online]. Available: <http://www.wvminesafety.org/sagointerviews.htm>
- [2] E. L. Checca and D. R. Zuchelli, "Lightning strikes and mine explosions," in *Proc. 7th US Mine Ventilation Symp.*, Jun. 5–7, 1995, pp. 245–250.
- [3] E. L. Checca, "Oak Grove mine methane gas ignition," U. S. Dept. Labor, Mine Safety, and Health Admin., Pittsburgh Safety and Health Technol. Center, Pittsburgh, PA, Investigative Rep. C-042094, Apr. 6–12, 1994.
- [4] D. S. Scott, E. L. Checca, C. R. Stephan, and M. J. Schultz, "Accident investigation report (underground coal mine) non-injury methane explosion," U.S. Dept. Labor, Mine Safety, and Health Admin. District 11, Oak Grove Mine, I.D. No. 01-00851, Jan. 29, 1996.
- [5] D. S. Scott and C. R. Stephan, "Accident investigation report (underground coal mine) non-injury methane explosion," U.S. Dept. Labor, Mine Safety and Health Administration, District 11, Oak Grove Mine, I.D. No. 01-00851, Jul. 11, 1997.
- [6] T. Novak and T. J. Fisher, "Lightning propagation through the earth and its potential for methane ignitions in abandoned areas of underground coal mines," *IEEE Trans. Ind. Appl.*, vol. 37, no. 6, pp. 1555–1562, Nov/Dec. 2001.
- [7] H. K. Sacks and T. Novak, "Corona discharge initiated mine explosion," in *Proc. IEEE Ind. Appl. Conf., 39th IAS Ann. Meeting Conf. Record.*, Oct. 3–7, 2004, vol. 2, pp. 1108–1114.
- [8] J. B. Liu, P. D. Ronney, and M. A. Gundersen, "Premixed flame ignition by transient plasma discharges," presented at the 29th Int. Symp. Combustion, Sapporo, Japan, 2002.
- [9] P. D. Ronney, "Technical progress report on corona discharge initiation," Univ. Southern California, Dept. of Aerosp. Mech. Eng., Los Angeles, CA, Rep. OSTI ID: 822386, Sep. 12, 2003.
- [10] K. Berger, *Protection of Underground Blasting Operations*, ch. 20, vol. 2, R. H. Golde, Ed. London, U.K.: Academic, 1977.
- [11] H. J. Geldenhuys, A. J. Eriksson, W. B. Jackson, and J. B. Raath, "Research into lightning-related incidents in shallow South African coal mines," in *Proc. 21st Int. Conf. Safety Mines Res.*, 1985, pp. 775–782.
- [12] P. Golledge, "Sources and facility of ignition in coal mines," in *Proc. Aus. I.M.M. Illawarra Branch, Ignitions, Explosions, Fires Coal Mine Symp.*, 1981, pp. 2-1–2-12.
- [13] H. J. Geldenhuys, "The measurement of underground lightning-induced surges in a colliery," presented at the Symp. Safety Coal Mining, South Africa National Electrical Engineering Research, Pretoria, South Africa, Oct. 5–8, 1987.
- [14] K. A. Zeh, "Lightning and safety in shallow coal mines," in *Proc. 23rd Int. Conf. Safety Mines*, 1989, pp. 691–700.
- [15] E. Petrache, F. Rachidi, M. Paolone, C. A. Nucci, V. A. Rakov, and M. A. Uman, "Lightning-induced voltages on buried cables—Part I: Theory," *IEEE Trans. Electromagn. Compat.*, vol. 47, no. 3, pp. 498–508, Aug. 2005.
- [16] E. Petrache, F. Rachidi, C. A. Nucci, V. A. Rakov, M. A. Uman, D. Jordan, K. Rambo, J. Jerauld, M. Nyffeler, and J. Schoene, "Lightning-induced voltages on buried cables—Part II: Experiment and model validation," *IEEE Trans. Electromagn. Compat.*, vol. 47, no. 3, pp. 509–520, Aug. 2005.
- [17] F. Delfino, R. Procopio, M. Rossi, F. Rachidi, and C. A. Nucci, "An algorithm for the exact evaluation of the underground lightning electromagnetic fields," *IEEE Trans. Electromagn. Compat.*, vol. 49, no. 2, pp. 401–411, May 2007.
- [18] M. B. Higgins and M. E. Morris, "Measurement and modeling of transfer functions for lightning coupling into the Sago mine," Sandia National Lab., Albuquerque, NM, SAND Rep. SAND2006-7976, 2007.
- [19] Staff-Mining Research, "Methane control in Eastern U. S. coal mines," presented at the Symp. Bureau Mines/Ind. Technol. Transfer Seminar, Morgantown, WV, May 30–31, 1973.
- [20] F. Clark, *Insulating Materials for Design and Engineering Practice*. New York: Wiley, 1962.
- [21] V. A. Rakov and M. A. Uman, *Lightning: Physics and Effects*. New York: Cambridge Univ. Press, 2003.
- [22] R. J. Fisher, G. H. Schnetzer, and M. E. Morris, "Measured fields and earth potentials at 10 And 20 meters from the base of triggered lightning channels," presented at the 22nd Int. Conf. Lightning Protection, Budapest, Hungary, Sep. 19–23, 1994.
- [23] J. Schoene, M. A. Uman, V. A. Rakov, V. Kodali, K. J. Rambo, and G. H. Schnetzer, "Statistical characteristics of the electric and magnetic fields and their time derivatives 15 m and 30 m from triggered lightning," *J. Geophys. Res.*, vol. 108, no. D6, pp. ACL6.1–ACL6.18, 2003.
- [24] M. A. Uman, D. K. McLain, and E. P. Krider, "The electromagnetic radiation from a finite antenna," *Amer. J. Phys.*, vol. 43, pp. 33–38, 1975.
- [25] R. Thottappillil, M. A. Uman, and V. A. Rakov, "Distribution of charge along the lightning channel: relation to remote electric and magnetic fields

and to return-stroke models," *J. Geophys. Res.*, vol. 102, pp. 6987–7006, 1997.

- [26] C. A. Nucci, G. Diendorfer, M. A. Uman, F. Rachidi, M. Ianoz, and C. Mazzetti, "Lightning return stroke current models with specified channel-base current: A review and comparison," *J. Geophys. Res.*, vol. 95, no. 20, pp. 395–408, 1990.
- [27] D. Rucker, M. Levitt, S. Calendine, J. Fleming, and R. McGill, "Geophysical survey for the old 2 left section of the Sago mine, Buckhannon, WV," hydroGEOPHYSICS, Inc., Tucson, AZ, 2006.
- [28] W. R. Smythe, *Static and Dynamic Electricity*. Albuquerque, NM: Summa Book, 1989.
- [29] V. A. Rakov and M. A. Uman, "Review and evaluation of lightning return stroke models including some aspects of their application," *IEEE Trans. Electromagn. Compat.*, vol. 40, no. 4, pp. 403–426, Nov. 1998.
- [30] V. Cooray, "Underground electric fields generated by the return strokes of lightning flashes," *IEEE Trans. Electromagn. Compat.*, vol. 43, no. 1, pp. 75–84, Feb. 2001.
- [31] J. R. Wait, *Electromagnetic Waves in Stratified Media*. New York: Macmillan, 1962.
- [32] J. A. Tegopoulos and E. E. Kriezis, *Eddy Currents in Linear Conducting Media*. New York: Elsevier, 1985.
- [33] R. L. Stoll, *The Analysis of Eddy Currents*. Oxford, U.K.: Clarendon, 1974.
- [34] A. Krawczyk and J. A. Tegopoulos, *Numerical Modeling of Eddy Currents*. Oxford, U.K.: Clarendon, 1993.
- [35] A. A. Kaufman and P. Hoekstra, *Electromagnetic Soundings*. New York: Elsevier, 2001.
- [36] D. A. Hill and J. R. Wait, "Subsurface electric fields of a grounded cable of finite length for both frequency and time domain," *Pure Appl. Geophys.*, vol. 111, no. 1, pp. 2324–2332, Dec. 1973.
- [37] E. Vance, *Coupling to Shielded Cables*. New York: Wiley, 1978.
- [38] L. K. Warne and K. C. Chen, "Long line coupling models," Sandia National Lab., Albuquerque, NM, SAND Rep. SAND2004-0872, 2004.
- [39] E. D. Sunde, *Earth Conduction Effects in Transmission Systems*. New York: Van Nostrand, 1949, pp. 112–272.
- [40] K. C. Chen and K. M. Damrau, "Accuracy of approximate transmission line formulas for overhead wires," *IEEE Trans. Electromagn. Compat.*, vol. 31, no. 4, pp. 396–397, Nov. 1989.
- [41] A. K. Agrawal, H. J. Price, and S. H. Gurbaxani, "Transient response of multiconductor transmission lines excited by a nonuniform electromagnetic field," *IEEE Trans. Electromagn. Compat.*, vol. EMC-22, no. 2, pp. 119–129, May 1980.
- [42] M. Rubinstein, "An approximate formula for the calculation of the horizontal electric field from lightning at close, intermediate, and long range," *IEEE Trans. Electromagn. Compat.*, vol. 38, no. 3, pp. 531–535, Aug. 1996.
- [43] V. Cooray and V. Scuka, "Calculation of induced voltages in power lines due to lightning-validity of various approximations," *IEEE Trans. Electromagn. Compat.*, vol. 40, no. 4, pp. 355–363, Nov. 1998.
- [44] C. A. Balanis, *Advanced Engineering Electromagnetics*. New York: Wiley, 1989.
- [45] M. A. Uman, private communication, 2006.
- [46] E. Philip Krider, private communication, 2006.



Matthew B. Higgins (S'97–M'08) received the B.S. and M.S. degrees in electrical engineering from The Ohio State University (OSU), Columbus, in 1999 and 2001, respectively, and the Ph.D. degree from the University of New Mexico, Albuquerque, in 2008.

From 1999 to 2002, he was a Graduate Research Associate with the ElectroScience Laboratory, OSU, where he was engaged in research in the area of ground penetrating radar and discrimination of buried unexploded ordnances and land mines. Since 2002, he has been with Sandia National Laboratories,

Albuquerque, where he is currently a Senior Member of Technical Staff with the Department of Electromagnetic Effects and is engaged in the electromagnetic (EM) qualification of two weapons systems for the Stockpile Lifetime Extension Program, electromagnetic code validation, FAA wiring diagnostics, the Sago mine disaster investigation, and research in EM coupling to multiconductor cables. He is currently the Chief Scientist for Special Programs in the Attach the Network tenant lane with the Joint Improvised Explosive Device Defeat Organization, Washington, DC.

Dr. Higgins is a member of Eta Kappa Nu.



Marvin E. Morris received the B.S. degree from New Mexico State University, Las Cruces, in 1965, the M.S. degree from the University of New Mexico, Albuquerque, in 1967, both in electrical engineering, and the M.S. and Ph.D. degrees from Harvard University, Cambridge, MA, in 1976 and 1977, respectively.

From 1965 to 1997, he was with Sandia National Laboratories, Albuquerque, NM. Since 1997, he has been working as a Consultant on similar topics for a variety of organizations. His current research interests include electromagnetic testing and analysis

problems related to effects of electromagnetic radiation, nuclear electromagnetic pulse, electrostatic discharge, and lightning on weapons.

Dr. Morris is a member of Eta Kappa Nu and a member of the Electrical and Computer Engineering Academy of New Mexico State University.



Michele Caldwell (M'01) received the Ph.D. degree in electrical engineering from Texas Tech University, Lubbock.

She is currently a Manager with the Department of Electromagnetic Effects, Sandia National Laboratories, Albuquerque, NM, where she is engaged in theoretical development, modeling and simulation, and experiments in a broad range of electromagnetic effects. Her research interests include lightning effects testing, systems engineering, and safety analyses.



Christos G. Christodoulou (F'02) received the Ph.D. degree in electrical engineering from North Carolina State University, Raleigh, in 1985.

From 1985 to 1998, he was a Faculty Member with the University of Central Florida, Orlando. He is currently a Professor with the Department of Electrical and Computer Engineering, University of New Mexico, Albuquerque, where he was the Chair from 1999 to 2005. He has authored more than 300 papers in journals and conferences, 12 book chapters, and has coauthored four books. His research interests

include the areas of modeling of electromagnetic systems, reconfigurable systems, machine learning applications in electromagnetics, and smart RF/photonics antennas.

Dr. Christodoulou is a member of Commission B of U.S. National Committee of the International Union of Radio Science (USNC/URSI), Eta Kappa Nu, and the Electromagnetics Academy. He was the General Chair of the IEEE Antennas and Propagation Society/URSI 1999 Symposium, Orlando, Florida, the Cochair of the IEEE 2000 Symposium on Antennas and Propagation for wireless communications, Waltham, MA, and the Co-Technical Chair for the IEEE Antennas and Propagation Society/URSI 2006 Symposium in Albuquerque. He is currently an Associate Editor for the *Antennas and Wireless Propagation Letters*, the *International Journal of RF and Microwave Computer-aided Engineering*, and the IEEE ANTENNAS and PROPAGATION MAGAZINE. He was appointed as an IEEE AP-S Distinguished Lecturer (2007–2009) and elected as the President for the Albuquerque IEEE Section in 2008. He was an Associate Editor for the IEEE TRANSACTIONS ON ANTENNAS AND PROPAGATION for six years, a Guest Editor for a special issue on "Applications of Neural Networks in Electromagnetics" in the Applied Computational Electromagnetics Society journal, and the Coeditor of the IEEE Antennas and Propagation Special issue on "Synthesis and Optimization Techniques in Electromagnetics and Antenna System Design" (March 2007).